Assignemnts for SF-AAA:
Civil GPS Jammer Geolocation From a UAV Using Received Signal Strength

AVDC 2018/2019 Course: SF-AAA Module

Dr Hyo-Sang Shin

Chapter 1

Introduction

A Global Navigation Satellite System (GNSS) such as the American Global Positioning System (GPS) has become prevalent in civilian applications and in the military. GNSS applications are numerous and varied as such systems provide accurate global positioning and time synchronisation. However one of GPS' primary weaknesses is its vulnerability to jamming as GPS signals coming from GPS satellites orbiting the Earth are extremely low-level signals at about -130 dBm as mentioned in [1].

A wide variety of civil GPS jammers are readily available on the market at affordable prices. As shown in [2], civil GPS Jammers are generally simple omni-directional monopole antennas with approximately fixed emitting power that sweep the main GPS band (about the L1 frequency at 1.57 GHz). Recent events such as thefts and airport incidents exposed this GPS vulnerability and growing jamming environment as shown in [3]. As a result, the authorities are taking steps to prevent their proliferation and try to develop GPS receivers robust to jamming as well as new means of detection and localisation of these jammers.

The passive localisation of Radio-Frequency (RF) emitters, also called geolocation, is a growing area of research thanks to the increasing use of Unmanned Aerial Vehicles (UAVs) in search & rescue and target tracking missions for both civil and military applications. These platforms have several advantages for geolocation including smaller platforms, more endurance and flexibility, team search and possible reduction in cost.

Geolocation using UAVs consists of three elements: measurements, estimation and guidance. It is a vast subject widely covered in the literature: numerous scenarios are possible in terms of measurement type, number of platform, fusion algorithm and guidance schemes. Examples of geolocation measurements include Angle of Attack (AOA) as in [4], Range and Time or Frequency Difference of Arrival (TDOA and FDOA respectively) as in [5, 6]. These measurements correspond to geometric curves in 2D that can be intersected over time or between various platforms. AOA (or bearing) corresponds to line-of-bearings (LOB) that intersect at the target position. This intersection is best obtained thanks to non-linear stochastic

filters such as Extended or Unscented Kalman Filter (EKF and UKF respectively). Geolocation scenarios are a result of a trade-off between estimation accuracy, complexity and cost. Those items stem mostly from choices in RF sensor, geolocation technique, number of platforms and fusion algorithm.

As civil GPS Jammer geolocation is a nascent issue, few papers address this problem. Couple papers investigate civil GPS Jammers characteristics [7] and in-car radiation patterns [7]. As for geolocation, some initiatives focus on the use of AOA which is one of the most accurate geolocation technique but it may be costly as it requires a complex antenna generally mounted on a gimbaled system for target tracking. [8] takes a different approach as it looks into the use of a network of ground vehicles fitted with RSSI sensor to produce a position estimate thanks to Differential Received Signal Strength (DRSS). This paper is particularly interesting as a RSSI sensor can be an inexpensive monopole GPS antennas. In that paper, an accuracy of 40m is demonstrated from tests. Yet, the requirement for a network of measurement platforms (e.g police vehicles) could be a hassle in terms of logistics and cost burden.

This assignment aims to investigate civil GPS Jammer geolocation using a single UAV fitted with a RSSI sensor. The solutions could address the cost concern while remaining logistically flexible with the advantage of the airborne platform being clear line-of-sight (LOS) with the target and greater area coverage. The main objective of this assignment is to develop a localisation algorithm in this specific scenario and bring the UAV onto a stand-off orbit around a stationary target, namely the GPS jammer, as it could be further identified.

Chapter 2

Assignment 1: GPS jammer geolocation in an ideal case

The models used in the first geolocation assignment are simple models . As the first step, let us consider an ideal case. Latter on, this case will be adapted to more complex models. First, simple assumptions and models used throughout this work are presented in the following sub-section.

2.1 Model Assumptions

Modelling assumptions concern primarily three items: environment, GPS Jammer and UAV.

A flat Earth model is adopted and the simulation is formulated in 2D as this provides good insight and the problem can be easily transferred to 3D. RF transmissions are assumed to happen in free-space and multipath considerations are dropped. It is an unusual choice in DRSS-based geolocation scenarios as a log-distance path loss model with correlated shadowing is generally preferred as in [8]. This assumption is motivated by the direct LOS with the target provided by the UAV and by the convenient use of the Frii's equation which explicitly includes gain distributions that can be measured in test chambers. Friis' equation of transmission is as follows:

$$\frac{P_r}{P_t} = G_t G_r \left(\frac{\lambda}{4\pi r}\right)^2 \tag{2.1}$$

where P_r, P_t, G_r, G_t are the received/transmitted power and receiver/transmitter gains respectively. λ is assumed to be the wavelength at the L1 frequency ($\lambda \approx$ 20cm) and r is the slant range between the UAV and the target.

The Civil GPS Jammer is first assumed to be *on the ground and static*. It has an unknown radiation pattern although equations are developed in the perfect isotropic case. Its signal characteristics (frequency, sweep scan) can be determined and remain constant. Its emitting power varies small enough to be assumed constant at P_t

(although this is questionable for Battery-powered devices). As represented in [2], Jammers are assumed to emit mainly around the L1 frequency about which they do linear sweeps to jam the GPS L1 band and their radiating power is constant. P_t ranges from milliwatts to more than half a Watt.

Finally the UAV platform is assumed to be small to medium sized (e.g 3 to 15 ft. wingspan) and is capable of accurate self-positioning in the GPS-degraded environment. Another preliminary assumption is that the sensor producing RSSI P_r is considered as isotropic with a unity gain $G_r = 1$ for the simplicity. The UAV model is also firstly simplified down to a 2D kinematic one as it can be easily steered in 2D:

$$\dot{\underline{s}} = \begin{pmatrix} \dot{x}_s \\ \dot{y}_s \\ \dot{h} \end{pmatrix} = V_g \begin{pmatrix} \cos(\psi) \\ \sin(\psi) \\ 0 \end{pmatrix} \tag{2.2}$$

where $\dot{\underline{s}}$ is the 3D absolute UAV position vector, h is the UAV altitude, V_g is the ground speed and ψ the UAV heading. This assumes that the UAV performs a level flight at altitude h_0. The altitude-hold and the other UAV dynamics are assumed to be taken care of by the flight control system. Finally, as in [9], the UAV heading is controlled to obtain the desired heading ψ^d. V_g and the turn rate command are both bounded: $V_{g,\min} \leq V_g \leq V_{g,\max}$ for minimum and maximum safe speed and $|\dot{\psi}| < \dot{\psi}_{\max}$ for minimum turn radius condition.

Power measurements using the antenna fitted on the UAV will be noisy. To assess noise levels, an approximate way is to consider thermal noise. A traditional formulation is the Johnson-Nyquist equation:

$$P_{\text{th}} = k_b \text{T B F} \tag{2.3}$$

where P_{th} is the thermal noise power, k_b is the Boltzmann constant, T the absolute temperature of the sensor sees (i.e the ground at $23°$), B the Jammer bandwidth and F is a factor to model " real " losses: typical values are 1 to 2 dB. A quick calculation yields $P_{\text{th}} \approx -100$ dBm with a bandwidth of 10 MHz and F = 2 dB. This noise level is particularly significant as GPS Jammers has low-power and will induce low signal-to-noise ratios S/N but it can be pre-filtered thanks to a low-pass filter.

Note that the received power with noises is already realised in the Matlab provided.

The search area is assumed to be a 12 km×12 km square with the Jammer randomly placed and oriented in a 4 km ×4 km square at the centre with the UAV placed at the South-West corner with a random heading. Its altitude is $h_0 = 200$ m and its speed is fixed at $V_g = 30$ m/s.

2.2   Geolocation Concept

RSSI measurements are usually used for range estimation. However Jammer powers vary greatly between retail models. Given one power measurement P_r, it is not viable to estimate range as this yields a ratio of approximately 25 between the maximum and minimum jammer power:

$$\frac{r_{\max}}{r_{\min}} = \sqrt{\frac{P_{t,\max}}{P_{t,\min}}} \approx 25 \tag{2.4}$$

Never-the-less, the DRSS geolocation technique can be developed using power ratios to cancel out the unknown variable P_t. Power ratios are equivalent to a log difference hence the name DRSS. Considering two power measurements at two different locations M_1 and M_2 in the search area, their ratio can be related to the true ranges ratio in the following way:

$$\frac{r_1^2}{r_2^2} = \frac{P_2}{P_1} = \alpha \tag{2.5}$$

This is possible because $P_t \left(\dfrac{\lambda}{4\pi} \right)^2$ is assumed constant for civil GPS Jammer and $G_t\,G_r$ remains constant (equal to unity in the simulation) as well with the isotropic assumption. From this, the Jammer lies on a geometric curve that corresponds to an " iso range-ratio ". The DRSS technique is well described in [10].

The following notation is adopted for clarity:

$$\underline{r} = \underline{x}_t - \underline{s} \tag{2.6}$$

with the Jammer being on the ground at:

$$\underline{x}_t = \begin{pmatrix} x_t \\ y_t \\ 0 \end{pmatrix}$$

From this, the slant range r is the module of $\underline{r}$ such that:

$$r = \sqrt{(x_t - x_s)^2 + (y_t - y_s)^2 + h_0^2} \tag{2.7}$$

Eqn. (2.5) can be developed using Eqn. (2.7) to get a circle Cartesian equation of "iso range ratio" as illustrated in [10]. The following provides a graphical explanation of the DRSS method.

For measurements at two positions of M_1 and M_2 and a power ratio α, the centre of this circle lies on the line $(M_1 M_2)$ at the centre C located at:

$$\underline{x}_c = \left[\frac{x_1 - \alpha\,x_2}{1 - \alpha} \,,\, \frac{y_1 - \alpha\,y_2}{1 - \alpha} \right] \tag{2.8}$$

Its radius is determined using Eqn. (2.9):

$$r_c^2 = x_c^2 + y_c^2 + \frac{\alpha(x_2^2 + y_2^2) - (x_1^2 + y_1^2)}{1 - \alpha} \qquad (2.9)$$

A special case happens when $\alpha = 1$ which corresponds to equal power measurements at M_1 and M_2. In that case, the circle becomes a line which is perpendicular to $(M_1 M_2)$ and passes through the Jammer. With the same assumptions as before, the equation of the line is:

$$
\begin{aligned}
y &= x\, \frac{x_1 - x_2}{y_2 - y_1} + \frac{(x_2^2 + y_2^2) - (x_1^2 + y_1^2)}{2\,(y_2 - y_1)} \quad ; \quad \text{if } y_2 - y_1 \neq 0 \\
x &= \frac{x_2^2 - x_1^2}{2\,(x_2 - x_1)} \quad ; \quad \text{otherwise}
\end{aligned}
\qquad (2.10)
$$

Note that, if $M_1 \approx M_2$, then the problem is undefined.

2.3 *Design of Filters (Assignment 1)*

The tasks for the first assignments are:

A1.a. Design a discrete EKF under assumption that the measurement is the power ratio α;

A1.b. Design a discrete UKF under assumption that the measurement is the power ratio α;

A1.c. Design a discrete PF under assumption that the measurement is the power ratio α;

A1.c. Compare the performance among the EKF, UKF, and PF designed and discuss about the results.

The purpose of the EKF and UKF is to obtain the Jammer position in the horizontal plane:

$$\underline{x}_k = \begin{pmatrix} x_k \\ y_k \end{pmatrix} \qquad (2.11)$$

where $\underline{x}_k$ denotes the position vector of the target in the horizontal plane at the time step k and consists of positions in x and y axes. The measurement equation is:

$$z_{i,k} = h_{i,k}(\underline{x}_k) + w_k \qquad (2.12)$$

where w_k is an additive Gaussian noise at the time step k. The non-linear measurement function $h_{i,k}$ is:

$$h_{i,k}(\underline{x}_k) = \alpha_{i,k} = \frac{P_{r,k}}{P_{r,i}} = \frac{r_i^2}{r_k^2} = \frac{\|\underline{x}_k - \underline{s}_i\|^2}{\|\underline{x}_k - \underline{s}_k\|^2} \qquad (2.13)$$

where $\underline{s}_i$ is the known UAV position vector at time i and r_i is the range between the UAV and Jammer at time i.

Power ratios are formed from a current measurement at M_k (numerator) and one other measurement at M_i that is assumed to be a reference (fixed denominator). To get the largest $\alpha_{i,k}$ variations, *please adapt $z_{i,k} = z_{1,k}$ in the assignment* (we will use notations of z_k, α_k or h_k for short to indicate $i = 1$). This implies that all measurements are always compared to those at the initial position M_1 in this assignment.

2.4   Guidance

In the assignments, guidance consists of two different phases: the first phase is defined as flyby phase and the second the vector filed guidance phase. As it will take some time for the proposed filters to converge, the UAV is flying on a given course. As you can see in the Matlab code provided, the UAV trajectory in the first phase is generated from so called "*the weaving path generation*", also called as "*winding path generation*. This is to get rid of "ghost" jammer which can be generated if the UAV flies in a straight line and increase observability. The second phase is the orbital adaptation which guides the UAV onto a stand-off orbit around the target. The applied guidance law in the second phase is called Lyapunov Vector Field Guidance (LVFG)

The LVFG guidance scheme is thoroughly presented in [9] and relies on Lyapunov stability theory to generate a desired vector field for the UAV. LVFG has the advantage of being tractable and easy to implement for stand-off orbit tracking. The orbital adaptation guidance architecture is conventional: the target position estimation is used by the LVFG to produce desired heading commands to the UAV. The UAV dynamics change its position for further measurements to be taken and analysed by the filter (see Figure 2.1).
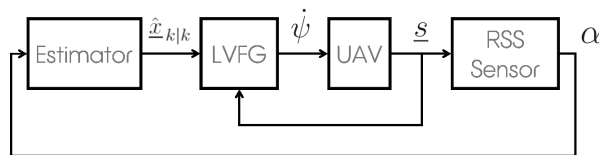

Figure 2.1: Block diagram of the orbital adaptation phase

Both the winding path generation and LFVG are realised in the provided code and you don't need to change anything in the guidance part of the code. However, note that the centre point of the stand-off orbit must be the estimate of the target position obtained from the filters you designed. Since you haven't developed any filter, the guidance schemes are implemented on the real target position. Therefore, when you design filters, you must replace this real target position by the estimated target position.

Chapter 3

Assignment 2:
GPS jammer geolocation under anisotropic Jammer pattern

So far, the target and UAV Antenna were assumed isotropic: same gains in all directions of space. However, these assumptions are invalid in reality. Therefore, it is required to take more realistic UAV and target models into account when one develops a geolocation method. The second assignment aims at solving the same geolocation scenario without the isotropy assumption for the GPS jammer, but retaining the UAV. The isotropic UAV antenna assumption for the time being. As a reminder, the jammer is still assumed static. The ideal model accuracy is correct but a more realistic approach needs to be adopted to more precisely model both the UAV and target.

3.1   More realistic models

The algorithm was developed with the assumption that the GPS Jammer has a constant gain G_t independent of direction. The isotropy assumption is relieved in this chapter because the target, namely a vehicle harbouring a GPS jammer, would have a highly anisotropic radiation pattern in reality. Indeed it can be understood that the GPS jammer will radiate omnidirectionally within the vehicle but the resulting RF energy will primarily " escape " through the windscreen and windows.

This was exposed during antenna gain measurements conducted by NSL. Numerous vehicles with GPS jammers at several different locations were tested and the global gain pattern was determined in an anechoic chamber. It underlines that radiation patterns may vary depending on the Jammer location inside the car. Moreover it may fluctuate as the Jammer sweeps in frequency or if the car vibrates as the engine is on or if the Jammer is battery-powered and the battery drains down. Figure 3.1 gives an idea of the anisotropic gain patterns dealt with in this project. This figure highlights strong angular variations of sometimes almost 30 dB in $5°$
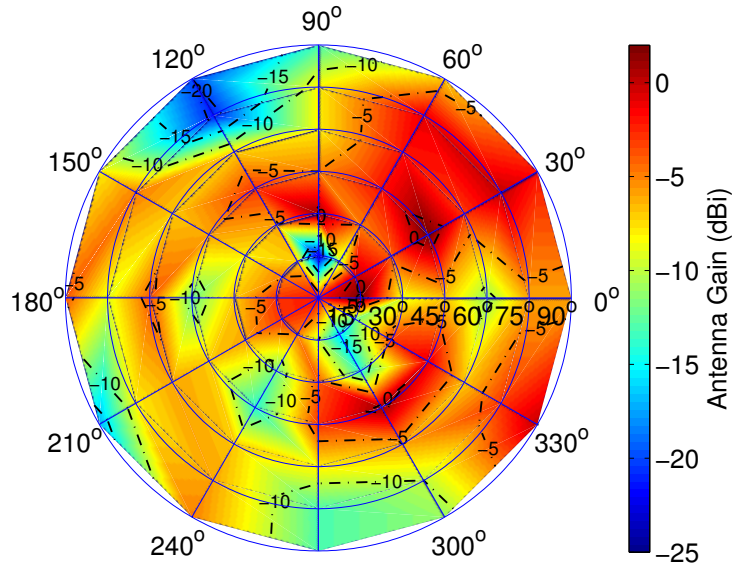
Figure 3.1: Illustration of possible jammer+vehicle gain patterns. This image is not representative of real tests. Azimuth angle is [0 - 360°], elevation [0 - 90°]

which represents a factor 1:1000 in power variations.

In the anisotropic jammer pattern case, G_t is assumed to be a function of azimuth and elevation, (ϕ, θ). Such a gain pattern is implemented into the simulation using a Simulink look-table. Depending on the current azimuth and elevation to the target, the corresponding gain is interpolated linearly in a table and given to the main algorithm of the Matlab code provided.

Of course this strong degradation is due to the anisotropy that disrupts the isotropic filter formulation. Indeed the power ratio $\alpha_{i,k}$ becomes:

$$\alpha_{i,k} = \frac{P_{r,k}}{P_{r,i}} = \frac{G_{t,k}(\phi_k, \theta_k)\, r_i^2}{G_{t,i}(\phi_i, \theta_i)\, r_k^2} \tag{3.1}$$

With time i being fixed (e.g $i = 1$), $G_{t,k}(\phi_k, \theta_k)$ makes the term $\dfrac{G_{t,k}(\phi_k, \theta_k)}{G_{t,i}(\phi_i, \theta_i)}$ become a source of noise on the current isotropic formulation. What is important to note is that this term is as noisy as $G_{t,k}(\phi_k, \theta_k)$ departs from the reference $G_{t,i}(\phi_i, \theta_i)$.

3.2 *Filter Design (Assignment 2)*

The tasks for the second assignments are:

A2.a. Analyse the performance of the EKF, UKF, and PF designed in Chapter 2 under the anisotropic jammer pattern;

A2.b. Design any filter algorithm which can alleviate the performance degradation results from the anisotropy;

A2.c. Analyse the performance of the proposed filter in A2.b and discuss about its results.

Bibliography

[1] A. Brown and D. Roberts. ammer and interference loca- tion system - design and initial test results. In *ION GPS '99*, 1999.

[2] B.W. O'Hanlon R.H. Mitch, M.L. Psiaki and S.P. Powell. Signal characteristics of civil gps jammers. In *ION GNSS 2012*, 2012.

[3] The economist. Gps jamming: No jam tomorrow, January 2013.

[4] K. Spingarn. Passive position location estimation using the extended kalman filter. *IEEE Transactions on Aerospace and Electronic Systems*, AES-23(4):558–567, 1987.

[5] F. Fletcher, B. Ristic, and D. Musicki. Recursive estimation of emitter location using tdoa measurements from two uavs. In *Information Fusion, 2007 10th International Conference on*, 2007.

[6] D. Musicki and W. Koch. Geolocation using tdoa and fdoa measurements. In *Information Fusion, 2008 11th International Conference on*, 2008.

[7] C. O'Driscoll D. Borio, J. Fortuny-Guasch. Characterization of gnss jammers. *Coordinates: A monthly magazine on position, navigation, and beyond*, May 2013.

[8] B. Eissfeller D. Fontanella, R. Bauernfeind. In-car gnss jammer localization with a vehicular ad-hoc network. In *the 25th International Technical Meeting of The Satellite Division of the Institute of Navigation (ION GNSS 2012)*, 2012.

[9] S. Morris E. W. Frew, D. A. Lawrence. Coordinated standoff tracking of moving targets using lyapunov guidance vector fields. *Journal of Guidance Control and Dynamics*, 31(2):290–306, 2008.

[10] Jeong Heon Lee and R.M. Buehrer. Location estimation using differential rss with spatially correlated shadowing. In *Global Telecommunications Conference, 2009. GLOBECOM 2009. IEEE*, pages 1–6, 2009.